

# Development of AMC Welding Wire and Inline Hot Rolling for Enhanced Properties of DED-Arc/Wire-Manufactured Parts

Tim Sebastian Tübbicke<sup>1,a\*</sup>, Fabian Dittrich<sup>1,b</sup> and Sebastian Härtel<sup>1,c</sup>

<sup>1</sup>Department Hybrid Manufacturing BTU Cottbus Senftenberg, Konrad-Wachsmann-Allee 17, 03046 Cottbus, Germany

<sup>a\*</sup>Tim.Tuebbicke@b-tu.de, <sup>b</sup>Fabian.Dittrich@b-tu.de, <sup>c</sup>Sebastian.Haertel@b-tu.de

**Keywords:** additive manufacturing, AMC, inline hot rolling.

**Abstract.** The wire arc directed energy deposition (DED-Arc/wire) process offers great potential for the additive manufacturing of large-volume components thanks to high deposition rates and cost-effective plant technology. Aluminium matrix composites (AMCs) are a high-performance alternative to conventional aluminium alloys, but their use in additive manufacturing has been limited so far due to porosity, restricted mechanical properties and a lack of semi-finished wire products. This paper presents a resource-efficient inline process chain for the additive manufacturing of silicon carbide-reinforced (SiC) AMCs (AMC-SiC). Since commercial AMC-SiC welding wires are not available, an AMC-SiC wire was produced from an aluminium tube (AW-6060) filled with AMC-SiC chips by means of multi-stage rotary swaging to a diameter of 1.6 mm. The DED-Arc/wire welding tests carried out demonstrate the basic processability of the developed wire, but with pronounced porosity in the weld seam. By integrating an inline hot rolling process, the weld bead was significantly deformed and the porosity was significantly reduced, thereby expanding the application potential of additively manufactured AMC-SiCs.

## Introduction

Additive manufacturing is a continuously growing manufacturing process that offers economic and ecological advantages over other manufacturing processes due to the possibility of saving material during component production [1-3]. In particular, the wire arc direct energy deposition (DED-Arc/wire) process offers the possibility of efficiently manufacturing larger components thanks to high deposition rates and cost-effective plant technology [2].

Conventional aluminium (Al) alloys often reach their limits in certain areas of application. These limitations can be reduced by using Al matrix composites (AMC), as these have excellent specific strength values, higher wear and temperature resistance, and lower thermal expansion [4]. The challenges in additive manufacturing, on the other hand, are reduced mechanical properties and an accumulation of pores in the resulting structure [5]. The production of an AMC-SiC welding wire and the inline hot rolling of the applied weld seam are intended to create a homogenised welding microstructure due to dynamic recrystallisation and closed pores [6]. This would significantly improve and expand the usability and range of applications of AMCs in the future.

The aim is to develop a resource-efficient inline process chain, which is primarily used for the targeted adjustment of the properties of silicon carbide-reinforced AMCs in AM. The AMC-SiC welding wire was manufactured in-house, as there is currently no AMC-SiC wire available on the market. AMC-SiC chip waste was used for this purpose. This has the advantage that it can be used directly and does not require energy-intensive melting to create the welding wire. In addition to this ecological advantage, process control and costs are significantly improved without the need for remelting. The AMC-SiC chips, measuring approximately 500 to 710 µm, were filled into a tube (AW-6060, dimensions 10 x 2 x 300 mm<sup>3</sup>) and then reduced to the required minimum diameter of 1.6 mm through rotary swaging in several stages.

## Material und Methodology

### Materials

As there is currently no commercially available AMC-SiC welding wire, the required wire was produced independently by the Department Hybrid Manufacturing (DHM) at the Brandenburg University of Technology Cottbus-Senftenberg (BTU). The starting point for production is silicon carbide-reinforced (SiC) AMC chips, which were provided by CMMC GmbH in Chemnitz, Germany. The AMC chips used consists of an AlSi9Mg alloy as a matrix and is reinforced with SiC with a grain size of F320 (29  $\mu\text{m}$ ) and a reinforcement content of approx. 20 % by volume. The initial structure of the AMC-SiC alloy used is shown in Figure 1.

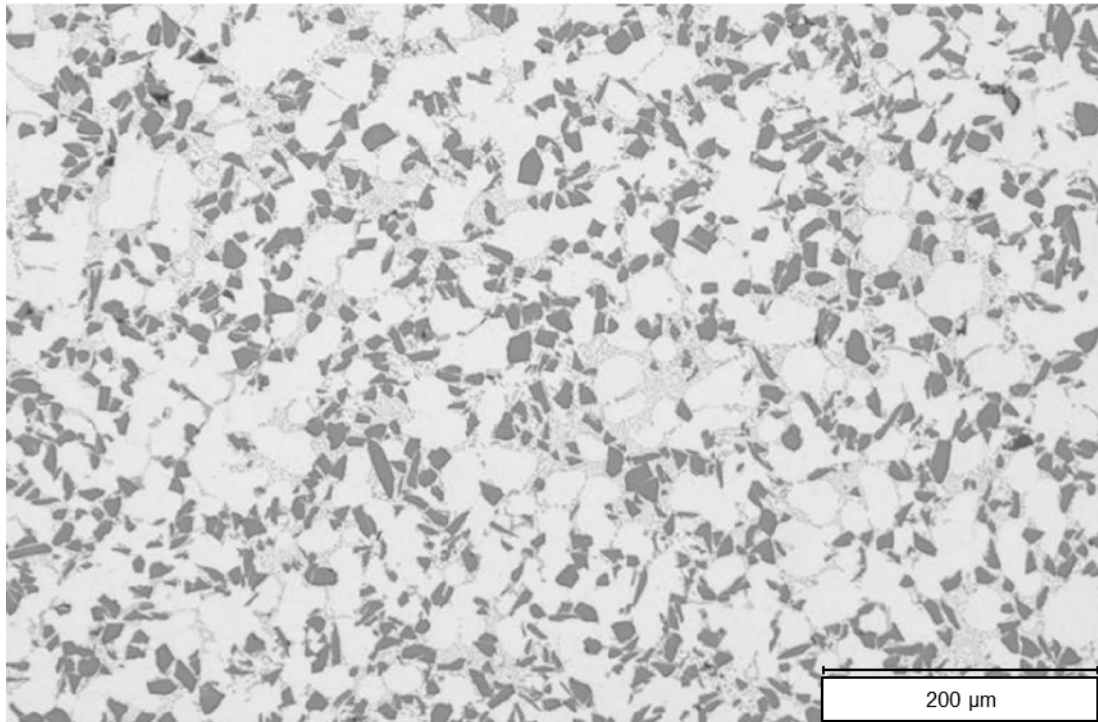


**Fig. 1.** Initial microstructure of the AMC alloy used, magnified 100 times.

These AMC-SiC chips are waste products from the machining of AMC-SiC semi-finished products. This approach aims to use the waste products from semi-finished products to produce welding wires without significant additional energy expenditure, which can then be used for the maintenance or repair of AMC components. The AMC-SiC chips used were not subjected to any pre-treatment, such as drying or similar. The reason for this was to be able to better examine the subsequent inline post-processing. The purpose is to produce a weldable AMC-SiC wire with a diameter of at least 1.6 mm from these AMC-SiC semi-finished products. In addition to the AMC-SiC material, an aluminium tube made of AW-6060 is also used to manufacture the wire, and all subsequent welding tests are carried out on a substrate plate made of AlMgSi0.5.

### Methodology

The FR 25 – VU rotary swaging machine from Felss Systems GmbH was used to manufacture the AMC-SiC welding wire. This machine makes it possible to gradually reduce the maximum diameter of 10 millimetres through forming. The forming steps are carried out in such a way that the diameter of the semi-finished product is reduced by approximately 9 % in each step.

The production of AMC-SiC welding wire based on the DFHs previous experience with self-manufactured filler wires for additive manufacturing [7] and is shown schematically in Figure 2.

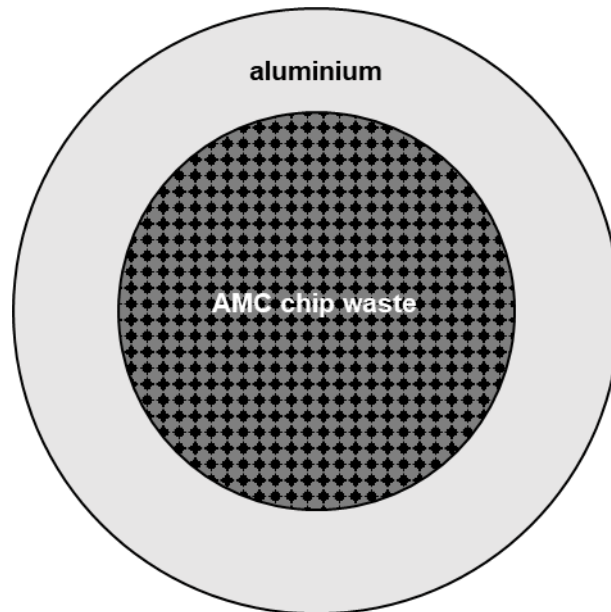


**Fig. 2.** Schematic illustration of the structure of AMC welding wire.

The recycled AMC-SiC chips were filled into an aluminium tube (AW-6060) measuring  $10 \times 2 \times 300 \text{ mm}^3$  and sealed at both ends. The size of the AMC-SiC chips ranged between 500 and 710  $\mu\text{m}$ . The forming took place in several steps up to a wire diameter of approximately 1.6 mm.

### Additive Manufacturing

The welding tests were carried out using a mobile pentapod from the company Metrom GmbH as the guide machine and connection point for the welding torch. Figure 3 shows the equipment used, including the pentapod.



**Fig. 3.** Equipment used for additive manufacturing.

The welding machine used was a Fronius tps400i. The welding tests with the manufactured AMC-SiC welding wire were carried out on a 10 mm thick aluminium substrate plate (AlMgSi0.5). An AlSi5 variant was used as the characteristic curve, as there is no explicit AMC-SiC characteristic curve available within the Fronius welding machine. The general welding parameters can be found in Table 1.

**Table 1.** Process parameters for additive manufacturing with AMC-SiC wire.

Welding parameters	Values	Units
Welding current	187	A
Welding voltage	15.3	V
Wire feed speed	5	m/min
Power	3.40	kW
Stickout	15 and 20	mm
Welding speed	400 and 600	mm/min
Shielding gas	100 % argon	
Welding wire diameter	1.6	mm

### Inline Hot Rolling

Inline hot rolling within the process chain is implemented using a specially manufactured rolling tool from the company Ecoroll AG. The rolling tool and its connection to the guide machine are shown in Figure 4.

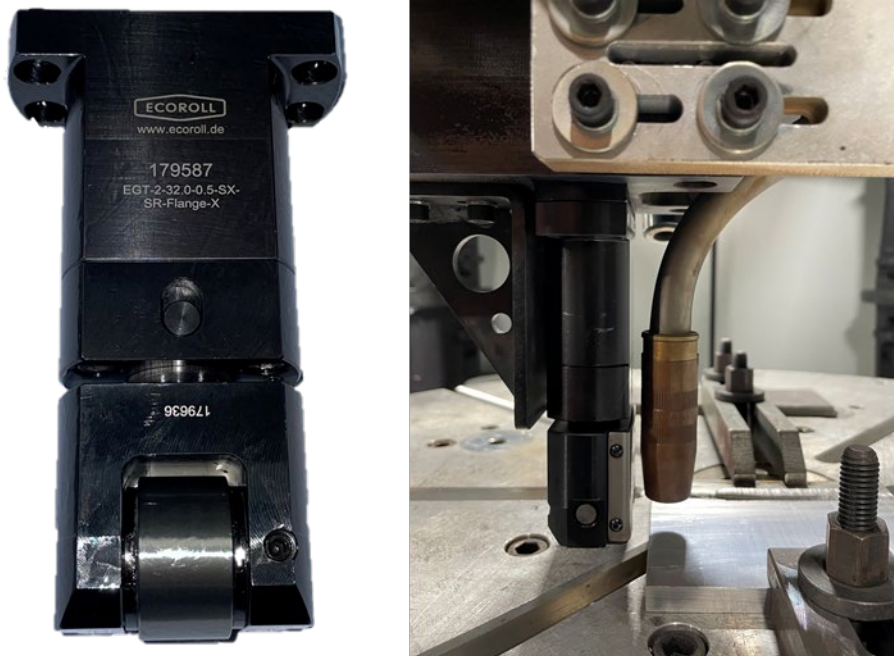


**Fig. 4.** Illustration of the rolling tool (left) and the inline process (right).

The rolling tool moves together with the welding torch and reshapes the resulting weld seam approximately 30 mm after application. Rolling forces of 4.5 to 11 kN can be set. The rolling force is generated via the spring deflection of the built-in disc springs and can be controlled via the stickout or the spacer plates between the tool and the system.

The inline reconsolidation process shown was carried out prior to welding with AMC-SiC welding wire using commercially available aluminium welding wire (AlSi10Mg). This was necessary due to the lack of AMC-SiC material. The preliminary tests are also considered in the results section.

### Material Characterization

The samples were ground (SiC grit #1200, #2000, and #4000) and polished (3  $\mu\text{m}$  diamond suspension and 0,025  $\mu\text{m}$  OPS solution) in multiple steps using a Struers Tegramin 30. The samples were investigated without etching using a Keyence VHX-7000 digital microscope and a Thermofisher Scientific Phenom XL Generation 2 tabletop SEM.

## Results

### AMC Welding Wire Production

The AMC-SiC welding wire could be manufactured without any restrictions. The minimum target diameter of 1.6 mm was achieved. A further reduction of the diameter to 1.2 mm was not pursued due to previous experience with other wires. The optical microscope analysis of the embedded AMC-SiC welding wire, shown in Figure 5, shows the inclusion of the AMC chips, including the SiC, in the manufactured wire.

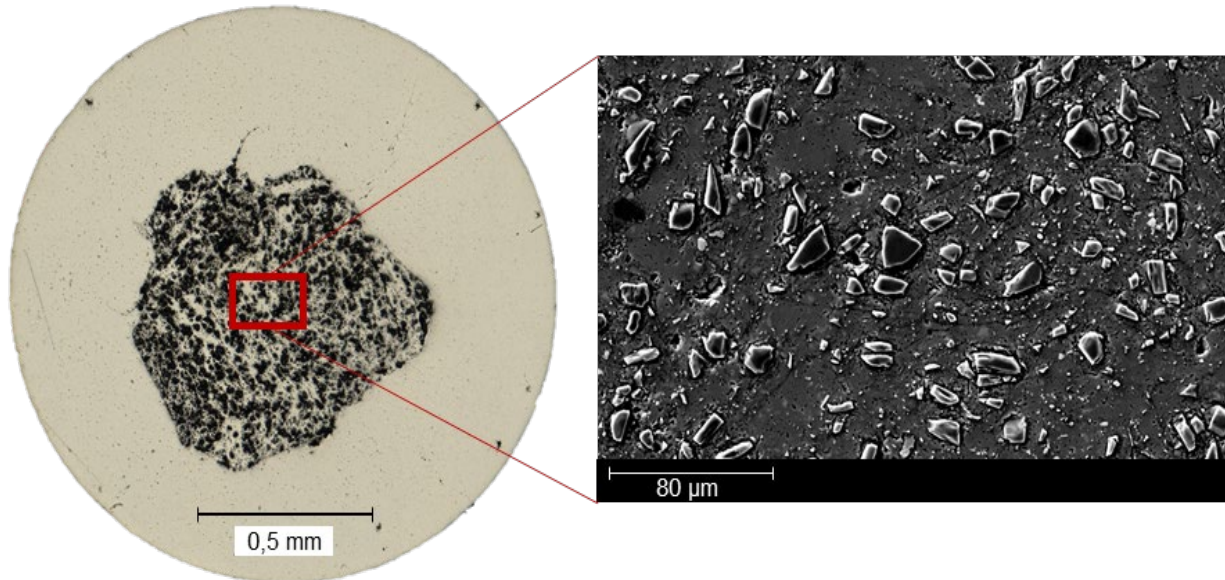


**Fig. 5.** Optical microscope examination of the manufactured AMC welding wire (left) and SEM analysis of the AMC material from inside the wire.

The SiC particles are clearly visible under the optical microscope. In general, the size of the particles has decreased slightly compared to the size in the AMC-SiC chips. The SiC particle size in the AMC chips was 20 to 30  $\mu\text{m}$ . The average particle size is smaller, but certain particles still reach the original size. The wire core surface area is roughly 25 % of the Al-mantle surface area, resulting in an approximately 8 % particle content in a successful AMC-SiC weld seam. This theoretically achievable strengthening phase content could be increased either by decreasing the mantle thickness and/or increasing the SiC-content in the base material chips.

A total of five AMC-SiC welding wires were produced in two different batches, as only enough AMC-SiC chips for two wires were available during the first wire production. Accordingly, the first batch was first welded completely and then the second batch was produced with new starting material. The total length of the welding wire available at the end was approximately 26 m.

### AMC Welding Test Series 1

The first welding tests with the self-produced AMC-SiC wire demonstrated the basic workability of the material combination. The general DED-Arc/wire process could be repeated without any process interruptions. During the process, there was significant spatter formation and a marked increase in smoke development. This indicates unstable molten pool control and potential gas release during the melting process. The resulting weld seam, which is shown in Figure 6, have irregular geometries and high porosity.

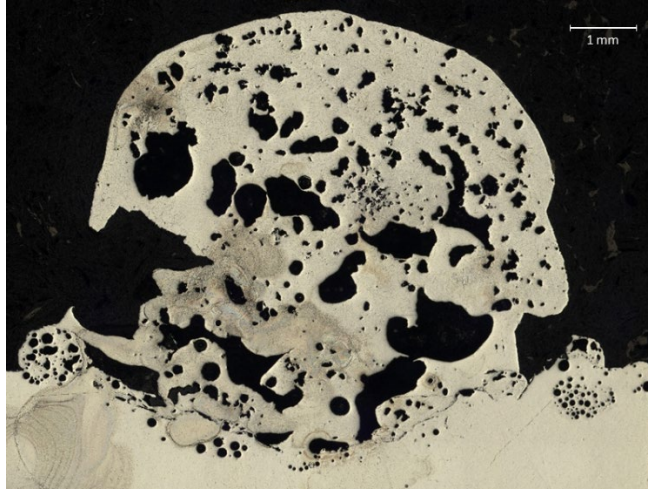


**Fig. 6.** Cross-section of the first AMC weld seam under the optical microscope.

A hydrogen analysis of the AMC welding wire showed a significantly increased hydrogen content compared to commercially available welding consumables such as AlSi10Mg, which was used in preliminary tests for inline hot rolling. This fact was initially accepted in order to better investigate the subsequent inline hot rolling process with the rolling tool. Extensive welding tests to optimize the welding parameters and thereby improve the weld seam results were not possible due to the limited amount of available material.

#### **AMC Welding Test Series 2**

In the second batch of AMC-SiC welding wire, three wires with a diameter of approx. 1.6 mm were produced. Hydrogen analysis of the wires shows a significant reduction in hydrogen content. This value was only three times higher than that of commercially available wire and thus only one tenth of the value of the other batch. This value was deliberately maintained in order to better investigate the expected improvement in the weld seam through inline hot rolling. Further hydrogen reduction through cleaning and drying of the recycled AMC-SiC chips would be possible and ultimately desirable. The reduced hydrogen content led to more stable process behaviour with fewer spatters and less smoke development during the welding test. The resulting seam, shown in Figure 7, has a slightly more uniform surface structure and is also slightly better in terms of shape than the comparison seams from batch 1.

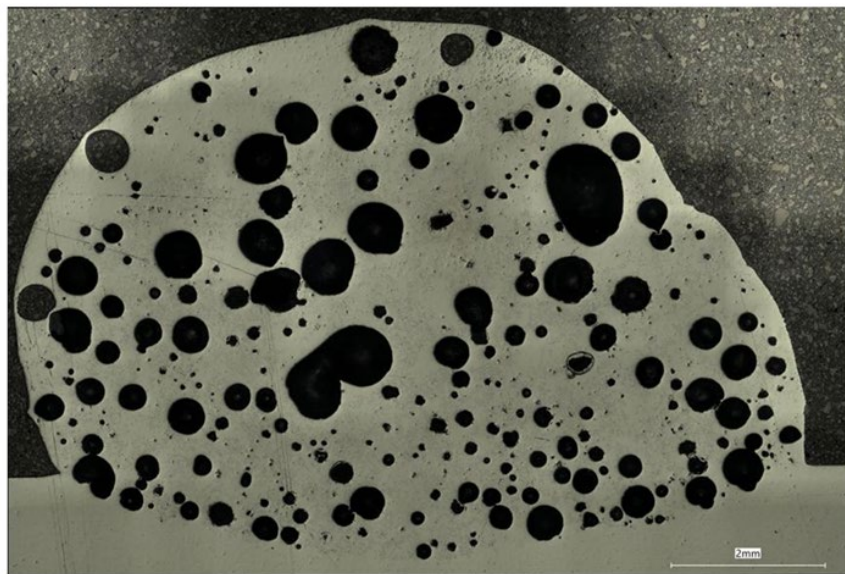


**Fig. 7.** Cross-section of the AMC weld seam produced with wire from batch 2 under an optical microscope.

The improved seam quality is related to the reduced hydrogen content of the wire, which indicates that the gas content in the starting material has a significant influence on process stability and seam formation. The observed result can be further improved with better pre-treatment of the starting material. The seam examined still has a hydrogen content three times higher than the reference seam. Careful variation of the process parameters through various welding tests with sufficient AMC-SiC welding wire would also help to further improve the welding result.

### Inline Hot Rolling Pre-Tests

Due to the limited availability of AMC welding wire, preliminary tests for inline hot rolling were carried out using a welding wire made from the Al alloy AlSi10Mg. This material is very similar to the matrix material of the AMC and is therefore well suited for preliminary tests.

Using the inline post-compaction method shown, the AlSi10Mg weld seams were formed immediately after application by the rolling tool. A comparison of the unrolled and rolled seams is shown in Figure 8.

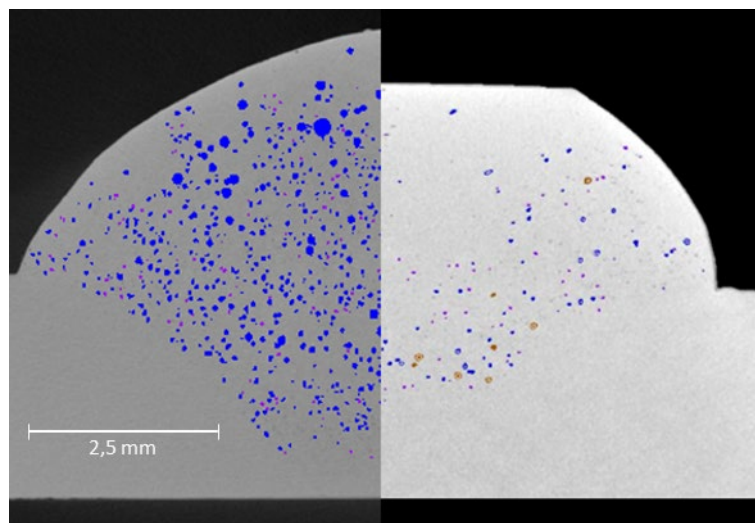


**Fig. 8.** Comparison of CT scans of the normal weld seam with the inline recompacted seam, including colored pore analysis.

The CT images clearly show that the porosity of the applied weld seam has decreased significantly, especially in the upper area of the seam. The porosity across the entire weld seam, of 50 mm, was reduced from approx. 5 % to around 1 % through inline hot rolling. This effect can also be seen in the fundamental simulation of inline hot rolling process in Figure 9.

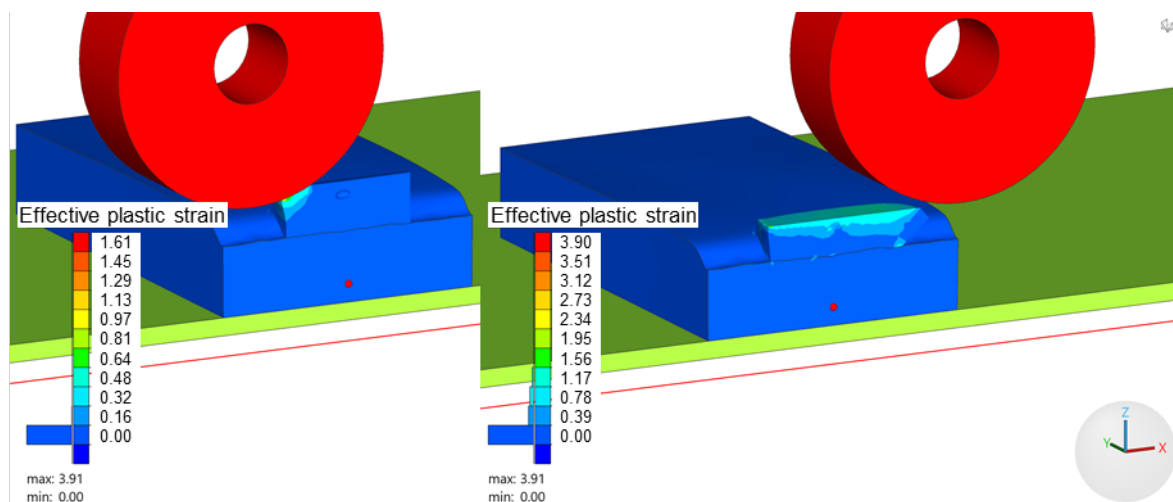


**Fig. 9.** Simulation result regarding the effective plastic strain of an comparable 50 mm aluminium weld seam.

Plastic deformation is at its highest directly below the surface. This leads to the pores close to the surface being closed in particular.

### Inline Hot Rolling with AMC Welding Wire

Inline hot rolling with AMC-SiC welding wire also worked. As can be seen in Figure 10, the percentage reduction in the height of the applied weld seam is significantly higher than in the preliminary test.

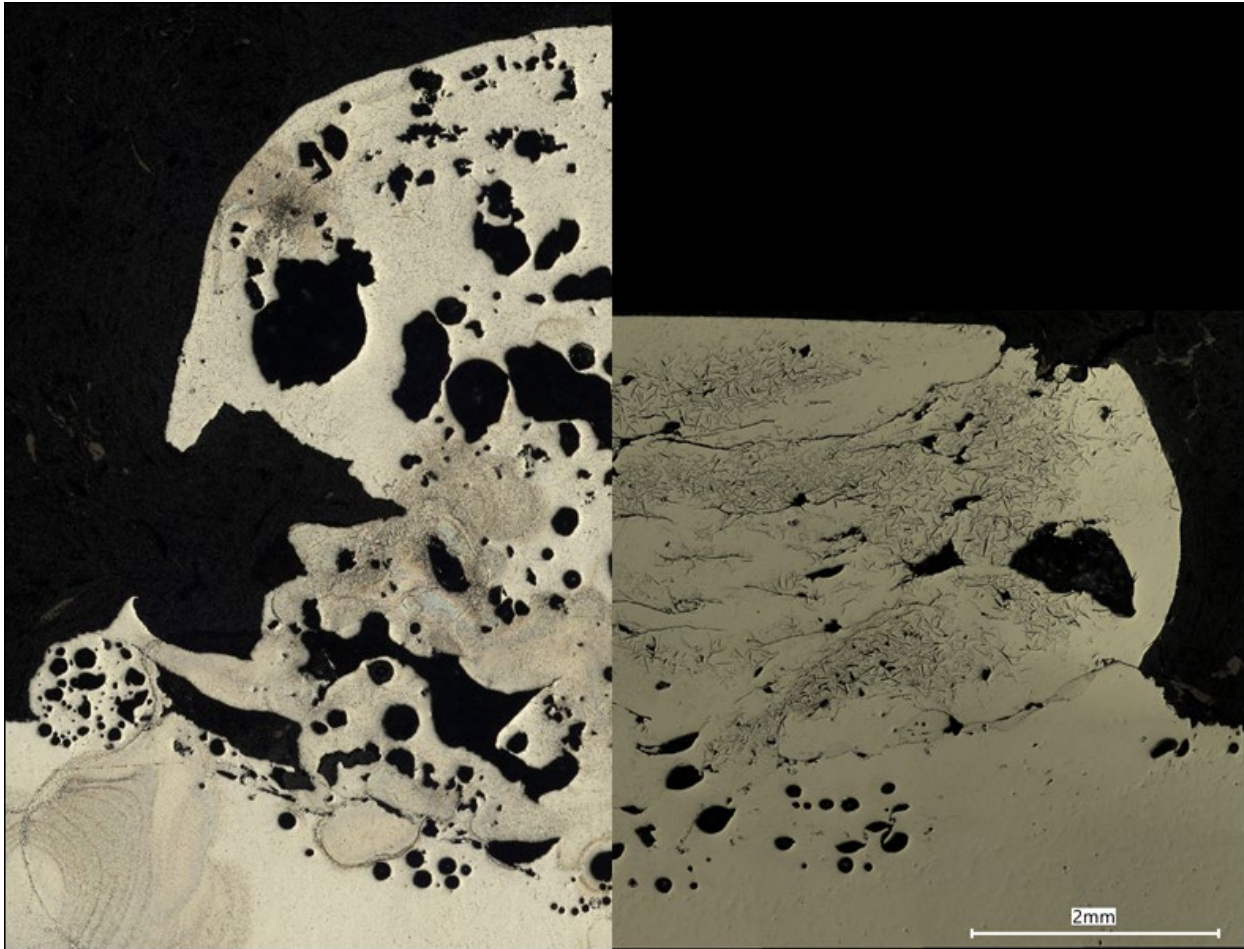


**Fig. 10.** Cross-section from optical microscope analysis – comparison of normal AMC weld seam (left) with inline recompacted weld seam (right).

This is mainly due to the porosity of the AMC-SiC weld seam. The rolling tool presses the seam more strongly through these larger pores, as there is less material present. Unfortunately, it was not possible to perform a comparative CT analysis of the porosity, as was done for the AlSi10Mg seam, because the evaluation software for porosity analysis was unable to examine the AMC-SiC seams. Nevertheless, the comparative image of the microscopic analysis of the cross-section shows that the porosity in the AMC-SiC weld seam is significantly reduced. Here, too, it can be seen that the compression is more pronounced in the upper part of the seam.

Even in the unetched state, distinct microstructural features were visible in all samples. Figure 11 illustrates needle-like features identified as a non-SiC phase throughout the matrix of the deposited material. The needles vary in length from 10  $\mu\text{m}$  up to 100  $\mu\text{m}$ , with a width of up to 10  $\mu\text{m}$  for the bigger needles. They are distributed mostly homogeneously through the matrix. Only in some samples, localized areas with fewer or no needles were observed.

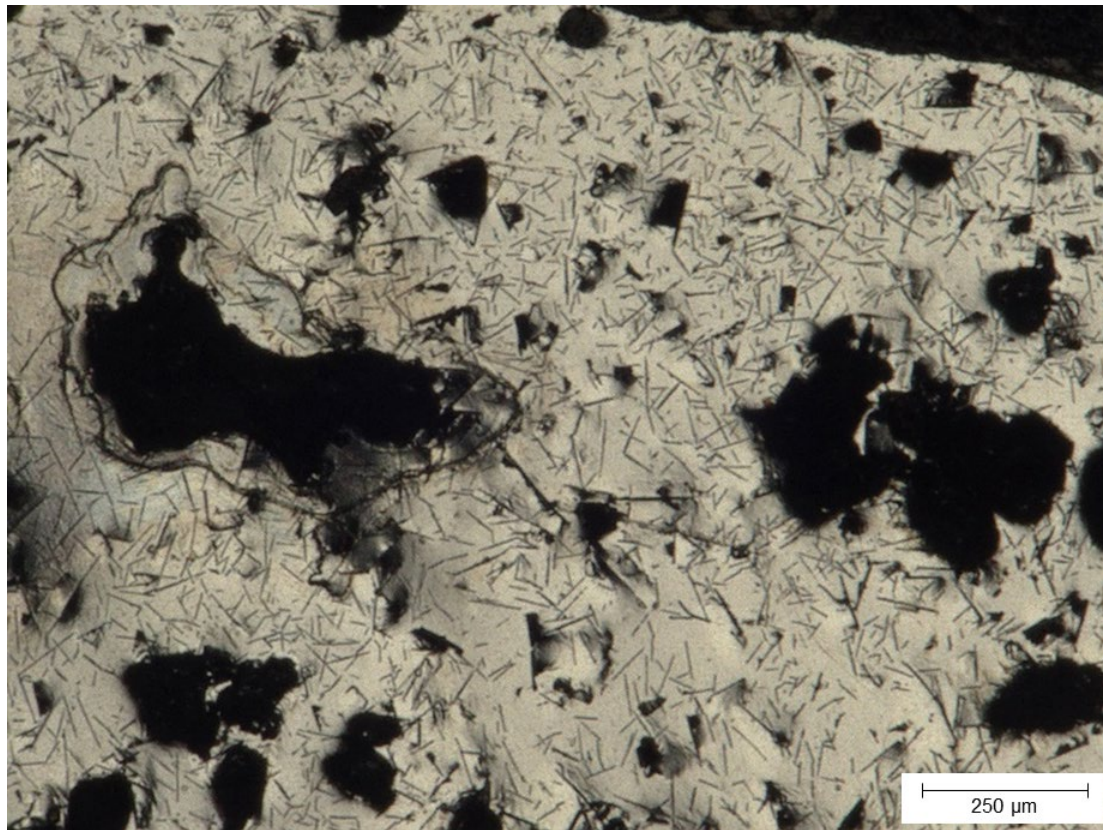


**Fig. 11.** Optical microscope image of the cross-section of an AMC weld seam.

Investigating these features with the SEM revealed the plate-like characteristic of the needle-shaped features in the matrix, see Fig. 12. The pore surfaces were covered with these plates, exhibiting various shapes, including dendrites and hexagons. EDS measurements on the needles/plates were not successful in identifying the phase. From a point measurement on a singular plate (indicated in Fig. 13 by a red arrow), it can just be assumed that the phase is a complex aluminum (30.6 at. %) silicon (2.3 at. %) carbon (25.9 at. %) oxygen (41.2 at. %) phase. Due to the small size of the plate, only low counts were registered in the detector over the 60-second measuring time, resulting in a rough estimate of the true composition of this phase only.

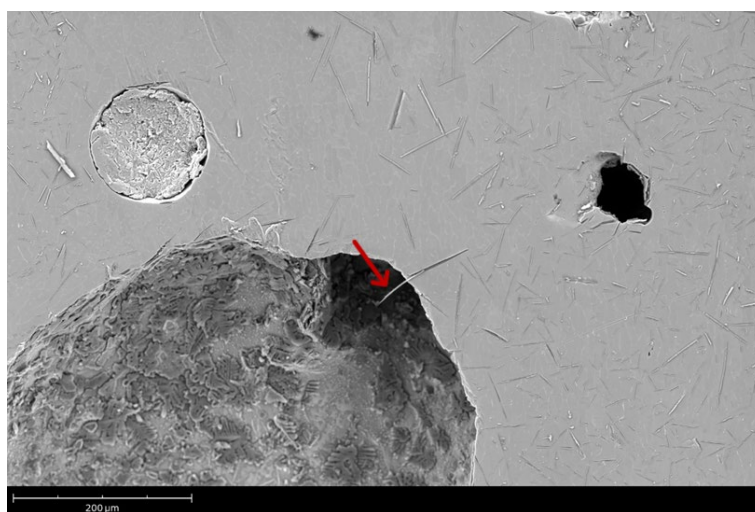


**Fig. 12.** SEM image of the cross-section of an AMC weld seam.

Moreover, next to no SiC particles were found in any of the samples. Only singular particles were found with sizes smaller than 10 μm (compared to the 20-30 μm measured in the base material/wire). Fig. 13 shows a former SiC particle likely during its dissolution during the process. Note that the former particle edge is lined with what appears to be the needle-like phase in the rest of the matrix.

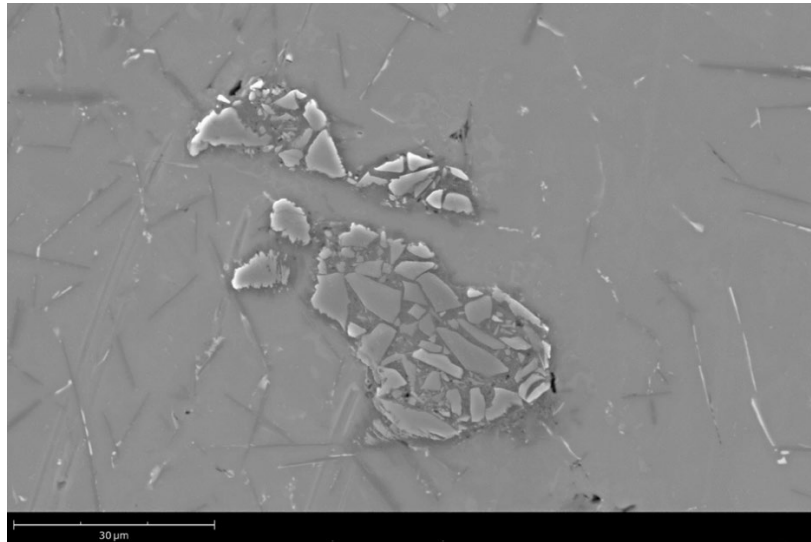


**Fig. 13.** Disintegrating SiC particle in an AMC welded seam.

The observed microstructure of the sample does not meet the expectation of a welded layer with an aluminum matrix reinforced with SiC particles. This finding is consistent with those of Xi et al. [8]. Their team investigated the processability of SiC reinforced AlSi10Mg via PBF-LB. They also report the disappearance of SiC after processing their base material. However, they did not discuss the reason for this observation. For this investigation, the dissolution of the SiC is likely a result of the process itself. Arc temperatures are reported to be higher than 6500 K [9]. Naturally, the processed material does not reach these temperatures, as that would mean that the material is starting to evaporate. However, melt pool temperatures exceeding 3000 K for short periods are realistic. Fig. 14 supports the idea that temperatures at least reach the decomposition temperature of SiC (3100 K [10]). The free silicon will readily dissolve in the aluminum matrix, while the free carbon has the potential to react with various partners, such as aluminum (forming aluminum carbide,  $\text{Al}_4\text{C}_3$  or  $\text{Al}_4\text{SiC}_4$ ), and aluminum oxide (forming  $\text{Al}_4\text{O}_4\text{C}$ ). Liu et al. break down possible chemical reactions in their study [11]. Assuming these interactions are applicable to this investigation, the disappearance of the SiC particles, as well as the appearance of another phase, could be explained.

### Summary and Forecast

The aim of this paper was to demonstrate the production and weldability of a SiC-reinforced AMC material. To this end, the manufacturing process for AMC-SiC welding wire was described, and a variant was developed that enables the production of weldable AMC-SiC welding wire with a diameter of 1.6 mm. The welding process with the AMC-SiC material was also successfully carried out in preliminary tests. The wires produced from the two different AMC-SiC welding wire batches had an increased hydrogen content, which result in unstable weld pool control and potential gas release. This circumstance was particularly pronounced in the first AMC-SiC welds and was already improved in the second batch, showing the importance of proper weld material preparation and handling. In order to improve the production and processability of AMC-SiC materials as welding consumables in the future, it is essential to optimize the properties of the raw materials used in the manufacturing process and then carry out larger-scale welding tests with the AMC-SiC wire in order to tailor the parameters of the DED-Arc/wire process to the material as closely as possible.

Future work will involve identifying the unknown phase using XRD. Furthermore, laser-based additive manufacturing methods may enable a process window where the temperature of the melt pool can be maintained below critical temperatures, thereby preventing the dissolution/decomposition of the SiC particles.

## Acknowledgement

The author gratefully acknowledges the support of the German Research Foundation e.V. (DFG e.V.), which enabled participation at ESAFORM 2026. The author also thanks colleagues and mentors for their valuable feedback and guidance during the preparation of this work.

## References

- [1] V. Pawlik, ‘Wie schätzen Sie die Entwicklungen auf dem Markt der Additiven Fertigung in den nächsten 24 Monaten ein?’, *statista*. Accessed: Dec. 03, 2025. [Online]. Available: <https://de.statista.com/statistik/daten/studie/1618955/umfrage/entwicklungen-additive-fertigung/>.
- [2] S. C. A. Costello, C. R. Cunningham, F. Xu, A. Shokrani, V. Dhokia, and S. T. Newman, ‘The state-of-the-art of wire arc directed energy deposition (WA-DED) as an additive manufacturing process for large metallic component manufacture’, *Int. J. Comput. Integr. Manuf.*, vol. 36, no. 3, pp. 469–510, Mar. 2023, doi: 10.1080/0951192X.2022.2162597.
- [3] ‘D Printing Trend Report 2024 Market growth, ecosystem maturation and technological innovations in 3D printing’, *Protolabs*, Maple Plain, USA, 2024. Accessed: Dec. 04, 2025. [Online]. Available: [www.protolabs.com/media/ktnlshstk/pl\\_3dp-trend-report-2024\\_en-2-1.pdf](http://www.protolabs.com/media/ktnlshstk/pl_3dp-trend-report-2024_en-2-1.pdf).
- [4] S. T. Mavhungu, E. T. Akinlabi, M. A. Onitiri, and F. M. Varachia, ‘Aluminum Matrix Composites for Industrial Use: Advances and Trends’, *Procedia Manuf.*, vol. 7, pp. 178–182, 2017, doi: 10.1016/j.promfg.2016.12.045.
- [5] M. Dadkhah, M. H. Mosallanejad, L. Iuliano, and A. Saboori, ‘A Comprehensive Overview on the Latest Progress in the Additive Manufacturing of Metal Matrix Composites: Potential, Challenges, and Feasible Solutions’, *Acta Metall. Sin. Engl. Lett.*, vol. 34, no. 9, pp. 1173–1200, Sep. 2021, doi: 10.1007/s40195-021-01249-7.
- [6] J. Huang et al., ‘Hybrid in-situ hot rolling and wire arc additive manufacturing of Al-Si alloy: Microstructure, mechanical properties and strengthening mechanism’, *J. Manuf. Process.*, vol. 127, pp. 328–339, Oct. 2024, doi: 10.1016/j.jmapro.2024.07.110.
- [7] A. Emdadi, S. Härtel, and A. Schmidt, ‘A holistic approach for near-net-shape processing of iron aluminides by means of Laser Directed Energy Deposition with cored wires’, presented at the 77th IIW Annual assembly and international conference on welding and joining, Rhodes, Jul. 2024, p. 6.
- [8] X. Xi, B. Chen, C. Tan, X. Song, and J. Feng, ‘Microstructure and mechanical properties of SiC reinforced AlSi10Mg composites fabricated by laser metal deposition’, *J. Manuf. Process.*, vol. 58, pp. 763–774, Oct. 2020, doi: 10.1016/j.jmapro.2020.08.073.
- [9] V. Babrauskas, ‘Electrical Fires’, in *SFPE Handbook of Fire Protection Engineering*, M. J. Hurley, D. Gottuk, J. R. Hall, K. Harada, E. Kuligowski, M. Puchovsky, J. Torero, J. M. Watts, and C. Wieczorek, Eds., New York, NY: Springer New York, 2016, pp. 662–704. doi: 10.1007/978-1-4939-2565-0\_22.
- [10] W. M. Haynes and D. R. Lide, Eds., *CRC handbook of chemistry and physics: a ready-reference book of chemical and physical data*, 92nd ed., 2011–2012. Boca Raton, Fla.: CRC Press, 2011.
- [11] J. Liu et al., ‘Fabrication, microstructure, and properties of SiC/Al<sub>4</sub>SiC<sub>4</sub> multiphase ceramics via an in-situ formed liquid phase sintering’, *J. Adv. Ceram.*, vol. 9, no. 2, pp. 193–203, Apr. 2020, doi: 10.1007/s40145-020-0359-8.